Radiation-Initiated Graft Polymerization of Methylmethacrylate onto Poly(tetrafluoroethylene): Characterization by ^{1}H-NMR

HIROSHI SAKURAI,[1] MASARU SHIOTANI,[1] HIDENORI YAHIRO[2]

[1] Department of Applied Chemistry, Faculty of Engineering, Hiroshima University, Higashi-Hiroshima 739-8527, Japan

[2] Department of Applied Chemistry, Faculty of Engineering, Ehime University, Matsuyama 790-8577, Japan

Received 12 October 1998; accepted 17 March 1999

ABSTRACT: A broad-line ^{1}H-NMR study was carried out to examine the local structure of poly(methylmethacrylate) (PMMA) grafted onto Poly(tetrafluoroethylene) (PTFE). The NMR spectra were observed for three different samples with 1.0, 5.4, and 7.0 wt % PMMA over the temperature range from 150 to 380 K. With the help of selectively deuterated PMMA (PMMA-d_5 and PMMA-d_8)-grafted samples, the NMR spectra were analyzed in terms of two components—a Gaussian (G) component, and a Lorentzian (L) component. Based on the second moments ($\langle \Delta H^2 \rangle$) analysis, the L and G components were attributed to the ^{1}H–^{1}H dipolar interactions within one CH_3 group and the interactions of CH_3 groups that are closely located in aggregated PMMA chains. Combining the results with the temperature dependence of $\langle \Delta H^2 \rangle$ and the angular resolved XPS, the location and rotational motion of PMMA grafted onto PTFE are discussed. © 1999 John Wiley & Sons, Inc. J Appl Polym Sci 74: 1386–1394, 1999

Key words: poly(tetrafluoroethylene); poly(methylmethacrylate); ^{1}H-NMR; deuteration; second moment

INTRODUCTION

Poly(tetrafluoroethylene) (PTFE) has attracted much attention and gained practiced use because of its outstanding properties, such as high thermal stability, low surface energy, and chemical inertness. The chemical inertness, however, makes it difficult to modify its surface without some pretreatment. Thus, surface modification of PTFE has been extensively studied with chemical treatment using alkali metals and organometallic reagents,[1,2] plasma treatment,[3–5] radiation treatment,[6–8] and physical treatment.[9,10]

For example, Hegazy and his coworkers reported that the radiation grafting of acrylic acid onto PTFE sheet resulted in significant improvement in swelling, water uptake, electron conductivity, and mechanical properties.[8] Yamada et al. have studied photograftings of acrylic acid and 2-(dimethyl amino)ethylmethacrylate onto plasma-treated PTFE sheet and found that its swelling property was much improved.[5] Thus, it has been reported so far that the PTFE surface is significantly improved by grafting various polymers onto it. However, little is known about the detailed nature of grafted polymers.

In the present study, selectively deuterated poly(methylmethacrylates) (PMMAs) were grafted onto pre-γ-irradiated PTFE with various grafting amounts. A broad-line ^{1}H-NMR spectroscopic method was applied to examine the local structure and dynamics of the grafted PMMA; the second moment (or spectral linewidth) should depend on both the rotational motions and the dis-

Correspondence to: M. Shiotani.

Journal of Applied Polymer Science, Vol. 74, 1386–1394 (1999)
 CCC 0021-8995/99/061386-09

tance and number of hydrogen atoms that are magnetically interacted with each other. Comparing the ^{1}H-NMR results with the angular resolved XPS results, we discuss the local structure and molecular motion of PMMA chains grafted onto the PTFE.

EXPERIMENTAL

Samples

PTFE powder (Daikin Co., Ltd.) was used as received. Methylmethacrylates used were $CH_2{=}C(CH_3)COOCH_3$ (MMA), $CD_2{=}C(CD_3)COOCH_3$ (MMA-d_5) and $CD_2{=}C(CD_3)\,COOCD_3$ (MMA-d_8) (Aldrich). They were dehydrated with molecular sieve 3A and purified by a vacuum distillation method to remove stabilizers before their use. PTFE powder (0.1 g) placed in a Pyrex glass tube (5 mm ∅) was degassed at 320 K for 1 h and then exposed to γ-rays (^{60}Co source) at room temperature with a total dose of 40 kGy. Two different radicals, —$CF_2\dot{C}FCF_2$— and —$CF_2CF_2\bullet$, were observed by ESR at 300 K. The latter radical was thermally less stable and was eliminated by annealing the sample at 400 K for 1 h; details will be given in the following section. The PTFE sample with —$CF_2\dot{C}FCF_2$— was then exposed to the MMA monomer (1.0 mL) at 273 K for various periods from 0.2 to 48 h. After grafting, the sample was stirred for 24 h in excess acetone followed by washing with the same solvent to remove unreacted MMA and PMMA homopolymer. The grafting amount was evaluated by thermogravimetry (TG) using SSC 5200 (Seiko Instruments) with a heating rate of 5 K/min.

Spectroscopy

The grafted samples were characterized using the following four different spectroscopic methods:

1. Single pulse ^{1}H broad-line NMR spectra were recorded with a Bruker AMX 400 spectrometer over the temperature range from 150 to 380 K. A sample of 0.1 g was evacuated at 300 K and sealed in a Pyrex glass tube. The $\pi/2$ pulse length was 4 μs with 1024 accumulations. Solid-state ^{13}C CP/MAS NMR spectra were measured using the same spectrometer for the samples of 200–300 mg in a rotor of ZrO_2. Magic angle spinning was executed at rates of approximately 4 kHz. The spectra were recorded using the following parameters: 6 μs of $\pi/2$ proton pulse length, 4 ms of contact time, and 1 s of delay time.
2. ESR spectra were measured with a Bruker ESP 300E spectrometer. The spectra were recorded at two different temperatures of 77 and 300 K, with a 100 kHz modulation amplitude of 0.32 mT and a microwave power of 1.0 mW.
3. FTIR spectra were recorded with a Perkin-Elmer SPECTRUM 2000 spectrometer over the wavenumber range of 4000–400 cm^{-1} with 4 cm^{-1} resolution at room temperature. Self-supporting thin films were used as samples, which were prepared by pressing a mixture of grafted sample and KBr powder with a volume ratio of 1 : 10 under a pressure of 300 kg cm^{-2} for 1 min.
4. XPS spectra were measured with a Perkin-Elmer Physical Electronics 5100 spectrometer using Mg K α excitation (400 W, 15.0 kV). The pressure in the analysis chamber was kept at 10^{-8}–10^{-9} torr during data acquisition. The spectra were recorded at several takeoff angles from 5° to 70° according to the method previously reported.[11] The atomic composition of the sample was evaluated using the following sensitivity factors: 1.00 for F_{1s}, 0.225 for C_{1s}.

RESULTS AND DISCUSSION

Evidence of PMMA Grafted onto PTFE

Figure 1(a) shows the ESR spectrum of γ-irradiated PTFE observed at 300 K together with the simulated one. The simulation was carried out by assuming two radical species, (I) and (II), with a relative intensity ratio of 1 (II)/4 (I): the ^{19}F hyperfine (hf) splittings used were (I) $A_{\parallel}(1\alpha\text{-F}) = 9.2$ mT, $A_{\perp}(1\alpha\text{-F}) = 3.4$ mT, $A_{\parallel}(4\beta\text{-F}) = 3.5$ mT, $A_{\perp}(4\beta\text{-F}) = 2.9$ mT, and (II) $A_{\parallel}(2\alpha\text{-F}) = 10.1$ mT, $A_{\perp}(2\alpha\text{-F}) = 2.5$ mT. Based on the ^{19}F hf splittings, radicals (I) and (II) were attributable to —$CF_2\dot{C}FCF_2$— and —$CF_2CF_2\bullet$, which were formed by ^{19}F atom detachment from the CF_2 group and skeletal C—C bond scission, respectively.[12] By annealing the samples at 400 K for 1 h, radical (II) decayed out irreversibly and radical (I) remained solely in the PTFE sample as shown in Figure 1(b). Immediately after introducing MMA to the annealed sample at 273 K, the ESR spectrum of radical (I) was almost replaced by that of a new radical whose spectrum consisted

of the following isotropic *hf* couplings: $a(CH_3)$ = 2.3 mT, $a(\beta\text{-H})$ = 1.4 mT, $a(\beta\text{-H})$ = 0.9 mT. The *hf* values are in fairly good agreement with those of the propagating radical of PMMA (see insert below).[13] The result clearly shows that radical (I)

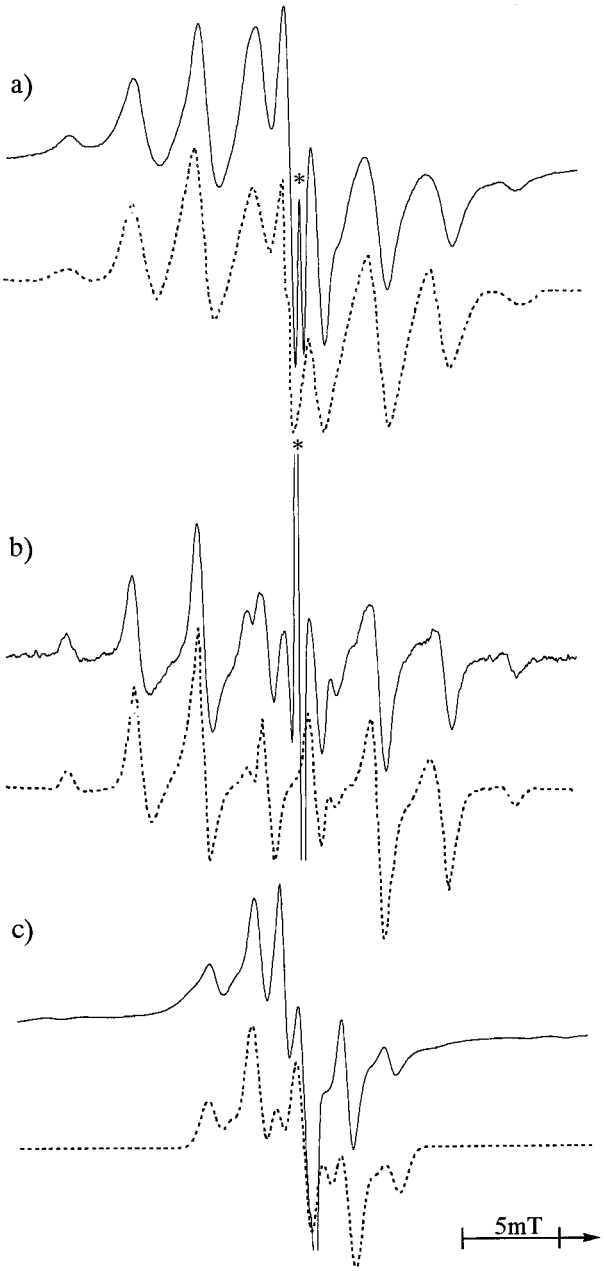

Figure 1 ESR spectra of PTFE powder; (a) After γ-irradiation at 300 K; (b) after subsequent annealing of (a) at 403 K; (c) immediately after the introduction of MMA to (b). Spectra (a) and (b) were recorded at 300 K, and (c) at 77 K. The signals marked with an asterisk (*) are due to damaged ESR sample tube. The spectra simulated to the experimental ones are given with the dotted lines. See details in text.

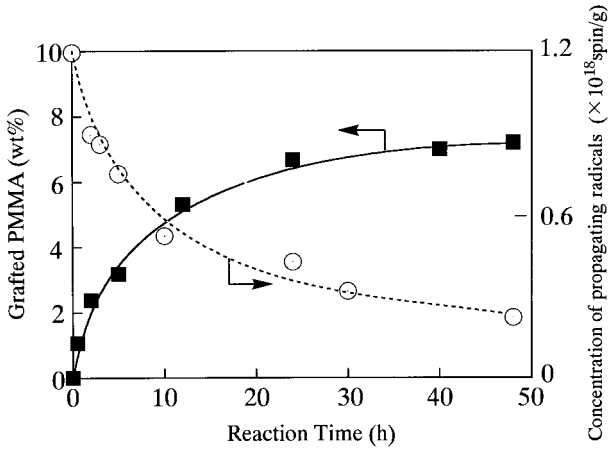

Figure 2 Amounts of PMMA grafted on PTFE (■) and the concentration of PMMA propagating radicals (○) are plotted against reaction time.

reacts with MMA monomers to give the propagating radical; a possible reaction scheme is given below:

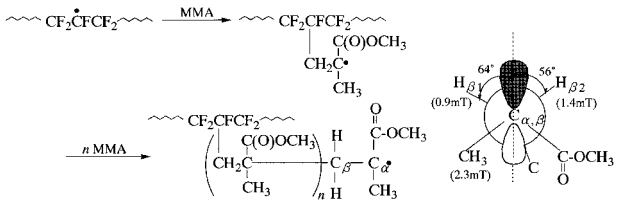

Insert 1

The formation of PMMA grafted onto PTFE (PTFE-*g*-PMMA) was confirmed by the following spectroscopic evidence: the FTIR spectrum of PTFE-*g*-PMMA showed the bands characteristic of PMMA at 1728 (C═O stretching vibration), 1500–1350 (C—H bending vibration), and 2989–2843 cm^{-1} (C—H stretching vibration).[14] ^{13}C CP/MAS NMR spectrum exhibited the signals due to the methyl group attached to the quaternary carbon (δ = 11.7 ppm), methylene carbon (46.2 ppm), methyl carbon attached to the carbonyl group (63.0 ppm), and carbonyl carbon (172.3 ppm).[15] Furthermore, the XPS spectrum gave four signals in the C_{1s} region, 292.0, 284.2, 285.9, and 288.1 eV, which were attributable to the carbons of PTFE, the methylene and/or methyl group, the C═O group, and the —OCH_3 group, respectively.[16]

Reaction Time Versus Grafting Amount

Figure 2 shows how the amount (wt %) of PMMA grafted onto PTFE increased with reaction time

after introducing the MMA monomer. The grafting amount was evaluated by thermogravimetry (TG), whose weight loss over the temperature range from 580 to 670 K was due to the decomposition of PMMA.[17] The amount increased with reaction time up to 40 h and then became almost constant. The number of reactive (radical) sites on PTFE, which were generated by γ-rays and measured by ESR, was kept constant in the present experiment. Thus, the increment of the grafting amount is responsible for that of the molecular weight, but not of the number of grafted PMMA chains. In Figure 2, the propagating radical concentration observed by ESR was also plotted against the reaction time. It can be seen from the figure that the propagating radical concentration decreased with reaction time due to either a recombination reaction or a disproportionation of the radical,[18] or both. The decrease in radical concentration should correspond to the decreased number of reaction sites toward new monomers. This can be a major reason why the leveling off was observed for the amount of PMMA grafted onto PTFE.

^{1}H-NMR Results

PTFE-g-PMMA and PTFE-g-PMMA-d$_5$

Figure 3(a) shows the NMR spectrum recorded at 340 K for the grafted sample with 7.0 wt % PMMA amount [PTFE-*g*-PMMA (7.0 wt %)]. The spectrum shows a broad linewidth of ca. 21 KHz due to dipolar interactions between various paired ^{1}H atoms; the broadening making it difficult to analyze the spectral lineshape. To have spectra with a narrower linewidth, MMA-d_5 was used as a monomer instead of normal MMA.

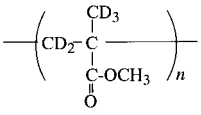

PMMA-d_5

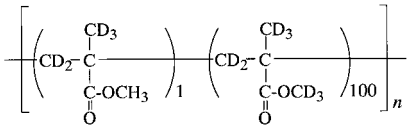

PMMA-d_5,d_8

Insert 2

Figures 3(b)–(d) represent ^{1}H-NMR spectra recorded at 340 K for PTFE-*g*-PMMA-d_5 with three different amounts of grafted PMMA—1.0, 5.4, and 7.0 wt %. It can be seen from the spectra that the linewidth becomes much narrower than that of the nondeuterated sample [Fig. 3(a)]. Furthermore, it was found that the spectra consisted of two components, a sharp one and a broad one, for

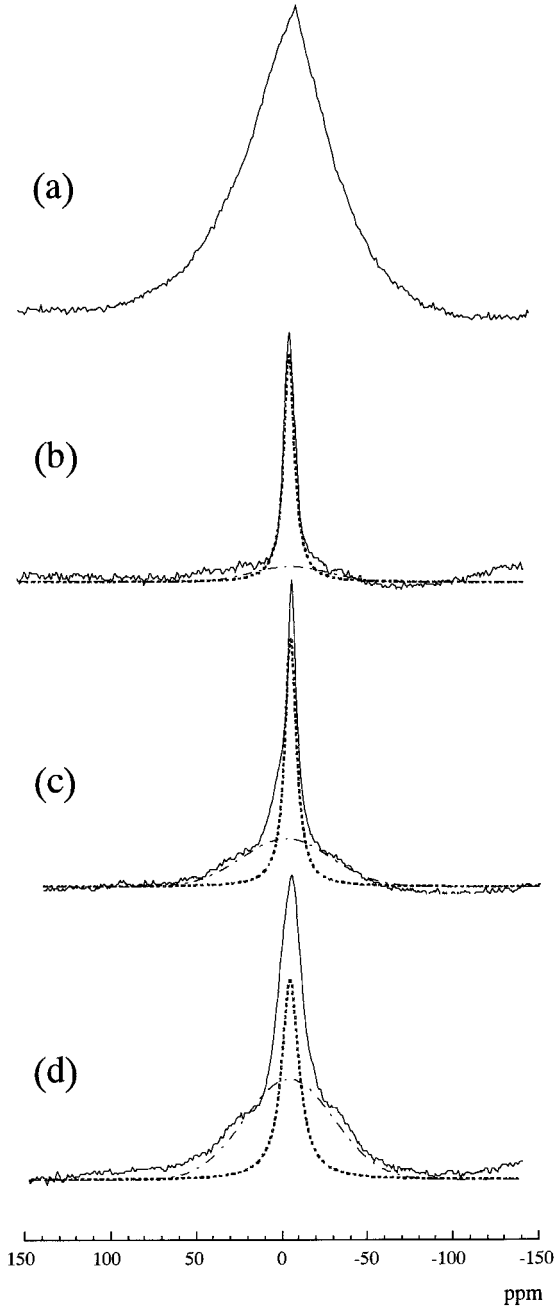

Figure 3 ^{1}H broad-line NMR spectra observed at 340 K for (a) PTFE-*g*-PMMA (7.0 wt %) sample recorded at 340 K. The spectra (b) to (d) correspond to PTFE-*g*-PMMA-d_5 samples with (b) 1.0 wt %, (c) 5.4 wt %, and (d) 7.0 wt % grafting amount, respectively. The experimental spectra were decomposed into a Gaussian lineshape (— - — -) and a Lorentzian lineshape (- - - - - - - -).

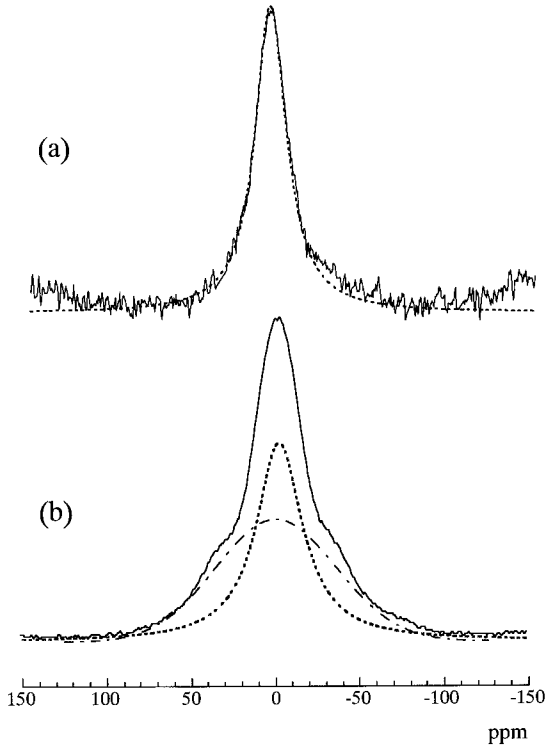

Figure 4 ^{1}H broad-line NMR spectra observed at 150 K for (a) PTFE-*g*-PMMA-d_5, d_8 (7.8 wt %) and (b) PTFE-*g*-PMMA-d_5 (7.0 wt %).

PTFE-*g*-PMMA-d_5. Obviously, the two components cannot be reproduced by either one Gaussian lineshape (G) or one Lorentzian lineshape (L). Instead, they were fairly well reproduced by employing the G lineshape for the broad component and the L lineshape for the narrow one, as shown in Figures 3(b)–(d). The second moments, $\langle \Delta H^2 \rangle$, of both the L and G components were evaluated and found to be almost independent of the grafting amount of PMMA (ca. 6 Gauss^2 for the G component, ca. 3 Gauss^2 for the L component at 340 K). The relative ratio (L/G) of the L component to G component, however, depended on the grafting amount, i.e., the L/G ratio decreased with increasing grafting amount; L/G = 3.0, 1.4, and 0.6 for 1.0, 5.4, and 7.0 wt % grafted PMMA, respectively. The results can be summarized as follows: (a) there exist two distinct local structures attributable to the L and G components for the PMMA grafted onto PTFE; (b) their local chemical environment is independent of the grafting amount. The G component increases more remarkably than the L component with the grafting amount.

PTFE-g-PMMA-d$_5$ Versus PTFE-g-PMMA-d$_5$, d$_8$

Possible magnetic dipolar interactions, which contribute to the L and G components, can come from pairs of ^{1}H–^{1}H and ^{1}H–^{19}F (^{19}F of PTFE); ^{1}H–^{2}D interaction should be negligibly small because of the 6.5 times smaller magnetic moment of ^{2}D than that of ^{1}H. To examine the difference in the dipolar interaction between the L and G components, a mixture of MMA-d_5 and MMA-d_8 with a mole ratio of 1 : 100 was grafted onto PTFE (see Insert 2); hereafter, this sample is called PTFE-*g*-PMMA-d_5, d_8. In Figures 4(a) and (b), the ^{1}H-NMR spectrum of PTFE-*g*-PMMA-d_5, d_8 (7.8 wt %) at 150 K is compared with that of PTFE-*g*-PMMA-d_5 (7.0 wt %). Interestingly, the spectrum of PTFE-*g*-PMMA-d_5, d_8 was found to be well reproduced by using solely one Lorentzian; the G component observed for PTFE-*g*-PMMA-d_5 completely disappeared in the spectrum. Based on the assumption that MMA-d_5 and MMA-d_8 monomer units are randomly mixed in PTFE-*g*-PMMA-d_5, d_8, the CH_3 groups are located at distances too far to magnetically interact with each other. Thus, we conclude that the G component observed for PTFE-*g*-PMMA-d_5 can predominately originate from the dipolar interactions between neighboring CH_3 groups (Insert 3), i.e., the ^{1}H–^{19}F dipolar interaction negligibly contributes to the linewidth. We attribute the G component to an aggregated local structure in which the CH_3 groups are located so close as to magnetically interact. Further discussions will be given in the following sections.

Temperature Dependence of the Second Moments

To obtain further information on the L and G components, temperature-dependent NMR spectra were measured for the PTFE-*g*-PMMA-d_5 samples with three different grafting amounts (1.0, 5.4, and 7.0 wt %). Figure 5 shows the spec-

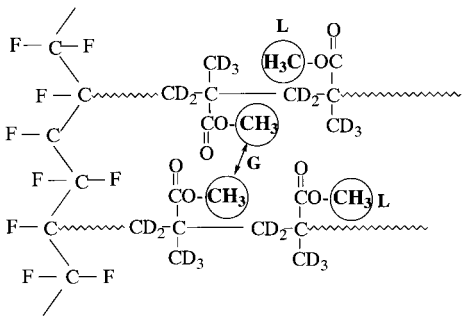

Insert 3

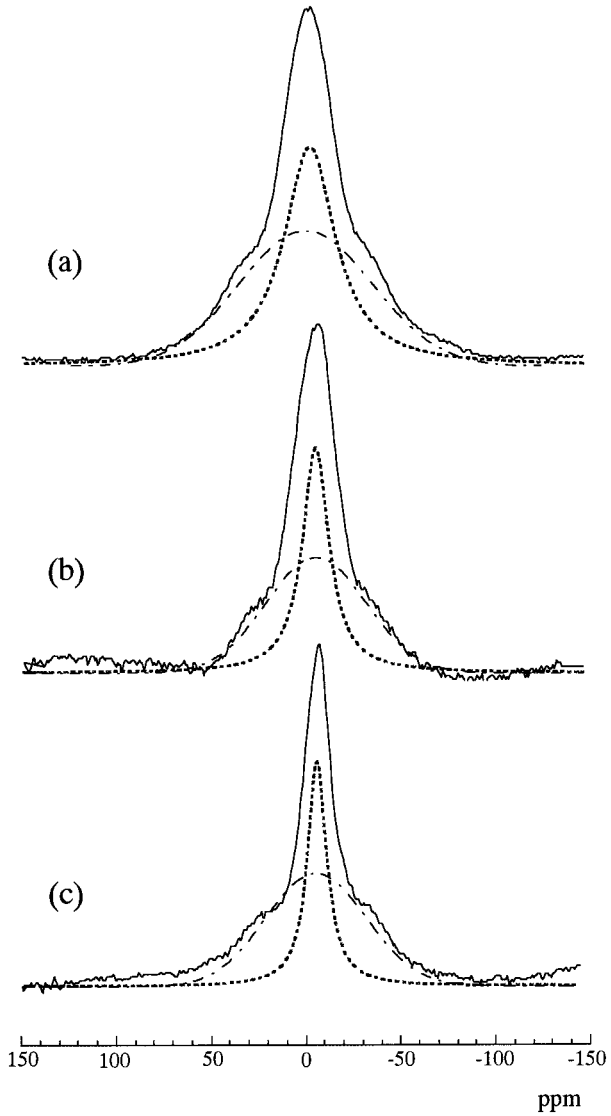

Figure 5 Temperature dependent ^{1}H broad-line NMR spectra of PTFE-*g*-PMMA-d_5 (7.0 wt %) recorded at (a) 150 K, (b) 240 K, and (c) 380 K. The experimental spectra were decomposed into a Gaussian lineshape (— - — -) and a Lorentzian lineshape (- - - - - - - -).

tra of a 7.0 wt % grafted sample observed at 150, 240, and 380 K. The spectra consisted of the L and G components, whose L/G ratio was 0.6, independent of temperature. The NMR spectra for 1.0 and 5.4 wt % samples also gave similar two components, but with smaller L/G ratio; the ratio decreases with the increment of the grafting amount (L/G = 3.0 and 1.4 for 1.0 and 5.4 wt % grafted PMMA).

The second moments, $\langle \Delta H^2 \rangle$, were evaluated for the three grafted samples and plotted as a function of measurement temperature in Figure 6. The values of $\langle \Delta H^2 \rangle$ were ca. 13 and 8 Gauss^2 for the G and L components at 150 K, respectively, which were independent of the grafting amounts. The values of $\langle \Delta H^2 \rangle$, however, decreased with increasing temperature so as to give ca. 6 and 3 Gauss^2 for the G and L components at 250 K, respectively; no appreciable temperature dependence was observed above 250 K.

When there exists only the interaction between identical nuclear spins (I), protons ($I = \frac{1}{2}$) in the present case, the $\langle \Delta H^2 \rangle$ can be expressed by the following equation[19]:

$$\langle \Delta H^2 \rangle = (\tfrac{3}{4}) g_N^2 \beta_N^2 I(I+1) n^{-1} \Sigma r_{j,k}^{-6} (1 - 3\cos^2\theta_{j,k})^2$$

where, g_N is the g value, β_N is the nuclear magneton, n is the number of protons, $r_{j,k}$ is the distance between protons j and k, and $\theta_{j,k}$ is the angle between the static magnetic field H_0 and the internuclear vector from proton j to k. The $\langle \Delta H^2 \rangle$ converges very rapidly because of its r^{-6} dependence. Thus, we may solely consider protons with shorter distances than 4 Å (which corresponds to $\langle \Delta H^2 \rangle$ = ca. 0.1 Gauss^2).

The $\langle \Delta H^2 \rangle$ of PTFE-*g*-PMMA-d_5, d_8 was 7.3 Gauss^2 at 150 K, which is very close to that of the L component of PTFE-*g*-PMMA-d_5 (7.0 wt %) (8.2 Gauss^2). The number of CH_3 groups in PTFE-*g*-PMMA-d_5, d_8 is 1/100 of that in PTFE-*g*-PMMA-d_5. This means that dipolar interactions among neighboring CH_3 groups in the former sample should be negligibly small. Almost the same second moments were observed for the former sample and the L component of the latter sample. Therefore, we attribute the $\langle \Delta H^2 \rangle$ of the L component to the ^{1}H–^{1}H dipolar interactions within one CH_3 group. Note that we can reasonably neglect the contribution from the interaction between ^{1}H and ^{2}D to $\langle \Delta H^2 \rangle$ because it is ca. two orders of magnitude less than the corresponding ^{1}H–^{1}H interaction.[20]

The theoretical $\langle \Delta H^2 \rangle$ values of the static (nonrotating) methyl protons and the freely rotating ones about the threefold (C_3) axis are 21.7 and 5.4 Gauss^2, respectively.[21] The $\langle \Delta H^2 \rangle$ values of both components at 150 K (ca. 13 and 8 Gauss^2) are much smaller than those of the isolated static CH_3 group, whereas the $\langle \Delta H^2 \rangle$ value of the L component (ca. 8 Gauss^2) at the same temperature is larger than that of the freely rotating CH_3 group. Admitting that the L component is due to the ^{1}H–^{1}H dipolar interactions within one CH_3 group, the rotational diffusion rate of the CH_3 group for PTFE-*g*-

PMMA-d_5 at 150 K is in the intermediate range between the static and the free rotations. Sinnott et al. reported that the CH_3 group attached to the ester groups in bulk PMMA is freely rotating at even 77 K.[22] However, in the present study, the same CH_3 group in PMMA grafted onto PTFE does not rotate completely freely. That is, the diffusion rate of the CH_3 groups in PMMA grafted onto PTFE is lower than that of the CH_3 groups in bulk PMMA. This indicates that the PTFE and PMMA chains interacted more strongly with each other than the bulk PMMA chains. In fact, a similar result has been reported in the spin labeling ESR study onto PMMA grafted on PTFE.[17]

The $\langle \Delta H^2 \rangle$ values of the G and L components above 250 K are ca. 6 and 3 Gauss^2, respectively. The difference of ca. 3 Gauss^2 can be attributed to the interaction of the CH_3 groups, which are closely located in aggregated PMMA chains, as previously mentioned. The $\langle \Delta H^2 \rangle$ values of the L component were independent of the grafting amounts, but decreased with increasing temperature from 150 to 250 K. We explain this as follows: the rotation rate increases with temperature up to that of the free rotation so as to give $\langle \Delta H^2 \rangle$ = 5.4 Gauss.^{2} The difference between the experimental value of $\langle \Delta H^2 \rangle$ = ca. 3 Gauss^2 (250 K $< T <$ 380 K), and 5.4 Gauss^2 may be responsible for the local motions of the ester group and/or microbrownian motion of the skeletal carbons. When the methyl group rotates about the C_3 axis, the term of $(1–3\ \cos^2\theta_{j,k})$ in the second moment can be expanded to: $\langle 1–3\ \cos^2\theta_{j,k} \rangle_{\text{avg}} = \frac{1}{2}(1–3\ \cos^2\theta')\ (3\ \cos^2\gamma_{j,k} - 1)$.

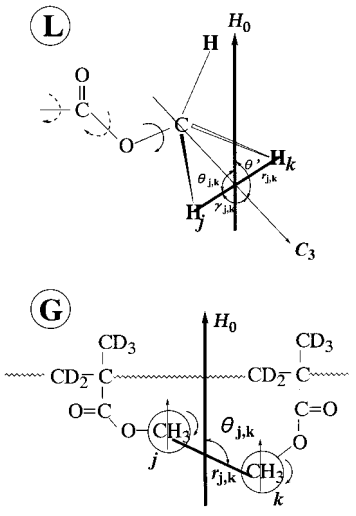

Insert 4

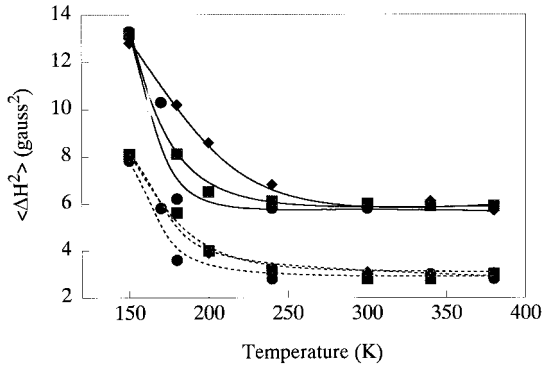

Figure 6 Plots of the second moment, $\langle \Delta H^2 \rangle$, against experimental temperature. The samples are PTFE-*g*-PMMA-d_5 with 1.0 wt % (●), 5.4 wt % (■), and 7.0 wt % (◆) grafting amounts.

where, the angle θ' and $\gamma_{j,k}$ are defined in Insert 4; in the present case, $\gamma_{j,k} = \pi/2$. Assuming that the $(1–3\ \cos^2\theta')$ is partially averaged by the motions, the $\langle \Delta H^2 \rangle$ value can be additionally reduced from the free rotation value.

Similarly, we can explain the temperature-dependent $\langle \Delta H^2 \rangle$ of the G component. In this case, the angle $\theta_{j,k}$ is redefined as shown in Insert 4. The rate of methyl group rotation increases with the temperature as before. At the same time, the $\theta_{j,k}$ term can be partially averaged so as to reduce the $\langle \Delta H^2 \rangle$, as observed.

L and G Components: A Model

It has been reported that PTFE powder is comprised of numerous particles with a diameter of ca. 0.1–0.4 μm called latex particles.[23,24] In fact, our SEM photograph of the PTFE powder used showed the existence of such latex particles. Rahl and his coworkers[24] have studied the polymer morphology of the latex particle by an electron diffraction method, and reported that the particle consists of thin lamella layers with ca. 3.3-μm length, ca. 0.3-μm width, and ca. 10-nm thickness, and is folded along the length direction in typical emulsion-grade materials prepared at Allied Chemical (see Insert 5).

Assuming that the molecular size of MMA (ca. 7 Å) is much smaller than that of voids among the folded lamella layers, MMA molecules may be diffused into the latex particle. Furthermore, the reactive radical sites are expected to be rather uniformly distributed in the latex particles. Thus, the polymerization of MMA may proceed at both the surface and the inside (or voids) of the latex particle.

Based on the amount of PMMA evaluated by the TG measurement and the number of radical sites on PTFE (1.2×10^{18} spins/g) by ESR, the average PMMA chain lengths per one radical site are estimated to be ca. 25, 140, and 180 nm for the 1.0, 5.4, and 7.0 wt % samples, respectively. The average chain lengths of the 5.4 and 7.0 wt % samples are comparable in size to the latex particle (ca. 0.1–0.4 μm). As previously mentioned, our NMR results suggested that the G component is attributable to a kind of aggregated PMMA in its local structure. The average PMMA chain length increased with reaction time after the introduction of MMA to the irradiated PTFE. The L/G ratios decreased with increasing average chain length. These suggest that the increment of the average chain length may give rise to an increase in the aggregated component. Thus, the PMMA chain in the latex is expected to be aggregated during the course of polymerization because the inside void diameter is expected to be much smaller than that of PMMA chain length. The PMMA may also reside on the surface of the latex particle. However, the amount should be much lower than that of the PMMA chain inside the latex because the outer surface area of the latex is negligibly small compared with the lamella surface area inside latex. On the other hand, for the 1.0 wt % grafted sample, the aggregation of PMMA chains in a latex particle did not proceed, because its average chain length (ca. 25 nm) may be short compared with the void size. In fact, the L/G ratio for 1.0 wt % grafted sample was 0.6, and the observed spectrum mostly consisted of the L component. A schematic model for the grafted sample is shown below.

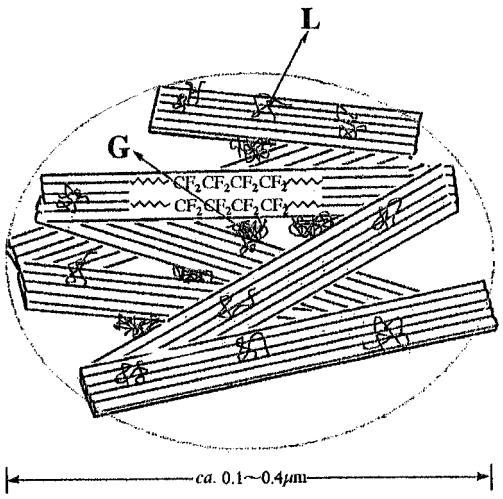

Insert 5

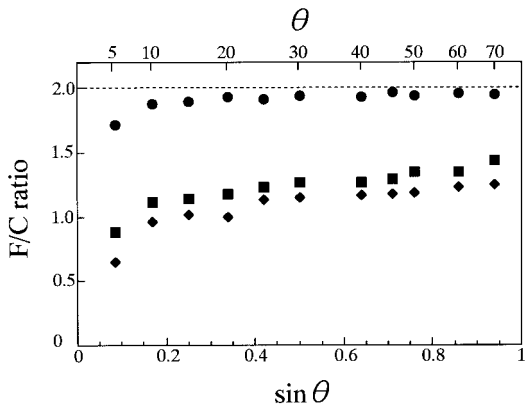

Figure 7 Plots of the F/C atomic ratios as a function of sin θ for PTFE-*g*-PMMA-d_5 samples with 1.0 wt % (●), 5.4 wt % (■), and 7.0 wt % (◆) grafting amounts.

Yamamoto and his coworkers[17] have studied the molecular motions of PMMA grafted onto PTFE by a spin-labeling ESR method. They reported that there exist two distinct PMMA components with lower and higher mobility; the former and latter were attributed to PMMA interacted with the PTFE surface and that located apart from the PTFE surface, respectively. They also reported that the former component was converted to the latter one with increasing temperature. Our NMR results also showed that there two components existed. However, no conversion takes place from G to L and/or L to G with increasing temperature; i.e., the grafting amounts of both components were independent of temperature. Thus, the present L and G components cannot be related to the two components derived from the spin-labeling ESR results.

Angular Resolved XPS Results

Angular resolved XPS measurements were carried out to have further experimental support for the conclusions derived from the ^{1}H-NMR results. The average atom composition along the depth direction of the polymer samples can be evaluated by changing the takeoff angle of the photoelectron, θ, with respect to the sample surface. The observed results are summarized in Figure 7. In the figure, the ratios of fluorides to carbons (F/C ratio) are plotted as a function of θ ($5° < \theta < 70°$) for the PTFE-*g*-PMMA samples with three different grafting amounts (1.0, 5.4, and 7.0 wt %). It is well known that the depth, where the photoelectron ejects from the sample surface, increases with increasing takeoff angle. Furthermore, the depth depends on the density of the sample used. The maximum depth obtained with $\theta = 70°$ cor-

responds to ca. 45 and 80 Å depths for pure PTFE (with a density of 2.18 g/cm^3) and PMMA (1.20 g/cm^3), respectively.[11] As the exact density is not available for the present PTFE-*g*-PMMA samples, we only know that the angle of $\theta = 70°$ corresponds to the depth between 45 and 80 Å. From Figure 7, we can observe the following: (a) the F/C ratio of the 1.0 wt % grafted sample is asymptotic to F/C = 2 (the ideal value of PTFE) at larger takeoff angles than 10°. (b) the F/C ratios of 5.4 and 7.0 wt % grafted samples are smaller than two at a $\theta = 70°$. The results suggest that the PMMA can be grafted onto both the surface and the inside of the latex particle. Especially the former indicates that most of the PMMA is located in the vicinity of the lamella surface for the low-grafting sample of 1.0 wt %. Whereas, the latter indicates that PMMA is located inside at least more than 45 Å from the surface of the latex particle when the grafting amount increases to more than 5 wt %. Thus, we confirmed that the XPS results were consistent with the NMR results showing that the aggregated PMMA can be mainly located in voids inside the latex particles.

CONCLUSIONS

A broad-line ^{1}H-NMR study of PMMA grafted onto PTFE was carried out to obtain information on the local structure of grafted PMMA chains. Employing MMA-d_5 and MMA-d_8 as a monomer, the associated NMR spectral linewidth drastically decreased, which enabled us to analyze the spectral lineshape. The observed spectra of PTFE-*g*-PMMA-d_5 consisted of two components, a Gaussian (G) lineshape and a Lorentzian (L) one, suggesting the existence of two different PMMA chains in the sample. Based on the $\langle \Delta H^2 \rangle$ analysis for PTFE-*g*-PMMA-d_5 and PTFE-*g*-PMMA-d_5, d_8, the L component was attributed to the ^{1}H–^{1}H dipolar interactions within one CH_3 group of PMMA, whereas, the G component was attributed to the interactions of the CH_3 groups that are in aggregated PMMA. The $\langle \Delta H^2 \rangle$ values were ca. 13 and 8 Gauss^2 for the G and L components at 150 K. Comparing these with the $\langle \Delta H^2 \rangle$ values of the static (21.7 Gauss^2) and freely rotating CH_3 group around the C_3 axis (5.4 Gauss^2), the CH_3 groups of both components attached to the ester groups in PMMA were concluded to be an intermediate rotational rate between them at this temperature. The same CH_3 group of bulk PMMA has been reported to be freely rotating at even 77 K.[22] This difference of the CH_3 group rotation can be attributed to a stronger interaction between the PTFE and PMMA chains than that between the PMMA chains. The $\langle \Delta H^2 \rangle$ values of the L and G components were independent of the grafting amounts, but the L/G ratio depended on the grafting amounts. Combining these results with the angular resolved XPS, we attributed the L component to the PMMA grafted onto the lamellas located near the surface of the latex particle; whereas the G component was attributed to that inside voids at least more than 45 Å of the surface.

The authors thank Mr. Yasuhiro Okuda, Sumitomo Electric Industry Co., Ltd. for helpful discussions.

REFERENCES

1. Rappaport, G. U.S. Pat. 2, 809 (1957).
2. Doban, R. C. U.S. Pat. 2, 871 (1957).
3. Hall, J. R.; Westerdahl, C. A. L.; Bodnar, M. J.; Levi, D. W. J Appl Polym Sci 1972, 16, 1465.
4. Wyderen, T.; Golubard, N. A.; Lerner, N. R. J Appl Polym Sci 1989, 37, 3343.
5. Yamada, K.; Hayashi, K.; Sakasegawa, K.; Onodera, J.; Hirata, M. Chem Soc Jpn 1994, 427.
6. Briscoe, B. J.; Evans, P. D. Wear 1989, 47, 133.
7. Hegazy, El-S. A.; Taher, N. H.; Kamal, H. J Appl Polym Sci 1989, 38, 1229.
8. Hegazy, El-S. A.; Ishigaki, I.; Rabie, A.; Dessouki, M.; Ahmed, Okamoto, J. J Appl Polym Sci 1981, 26, 3871.
9. Cirlin, E. H.; Kaelble, D. H. J Polym Sci Polym Phys Ed 1973, 11, 785.
10. Niino, H.; Yabe, A. Appl Surface Sci 1996, 96, 550.
11. Yamada, Y.; Yamada, T.; Tasaka, S.; Inagaki, N. Macromolecules 1996, 29, 4331.
12. Tamura, N. J Chem Phys 1962, 37, 479.
13. Komatsu, T.; Seguchi, T.; Kashiwabara, H.; Shoma, J. J Polym Soc C 1967, 16, 535.
14. Pouchert, J. C. The Aldrich Library of Infrared Spectra; Aldrich Chemical Company Inc.: Milwaukee, WI, 1981, p. 1164.
15. Schaefer, J.; Stejskal, E. O.; Buchdahl, R. Macromolecules 1977, 10, 384.
16. Girardeaux, C.; Idrissi, Y.; Pireaux, J. J.; Caudano, R. Appl Surface Sci 1996, 96, 586.
17. Yamamoto, K.; Shimada, S.; Tasaka, S.; Tsujita, Y.; Sakaguchi, M. Macromolecules 1997, 30, 1776.
18. Kausch, H. H. Polymer Fructure; Springer Verlag: Berlin, 1978; p 189.
19. Slichter, C. P. Principles of Magnetic Resonance; Springer Verlag: Berlin, 1978; p 70, vol. 1.
20. Andrew, E. A.; Eades, R. G. Proc R Soc (Lon) 1953, A218, 537.
21. Yukitoshi, T.; Suga, H.; Seki, S.; Itoh, J. J Phys Soc Jpn 1957, 12, 5068.
22. Sinnott, K. M. J Polym Sci 1960, 42, 3.
23. Symons, N. K. J. J Polym Sci Part 1 1963, 1, 2843.
24. Rahl, F. J.; Evanco, M. A.; Fredericks, R. J.; Reimschuessel, A. C. J Polym Sci Part A-2 1972, 10, 1337.